Soft Matter

PAPER

View Article Online
View Journal | View Issue



Cite this: *Soft Matter*, 2026, **22**, 449

# Mechanisms of abrupt fracture transitions in crystallizable elastomers

Zehao Fan, Fengjia Liu and Shi-Qing Wang *

We carried out theoretical analysis and experimental investigations to update our understanding concerning rupture and fracture transitions in continuous stretching of vulcanized natural rubber (NR). Besides a previously reported rupture transition in notch-free NR as a function of test temperature, we predict and confirm at elevated temperatures the existence of a rupture transition with respect to the applied stretch rate. In addition to the previously observed fracture transition in prenotched NR with respect to notch size, we also predict and observe two other transitions when either stretch rate or temperature is varied. For the first time we explain, based on our recently proposed kinetic theory of bond dissociation (KTBD) for elastomeric rupture and fracture, why these five transitions are abrupt with respect to the three variables of notch size, stretch rate and temperature for both unnotched and prenotched NR. Since the transition is determined by whether strain induced crystallization (SIC) in NR occurs – SIC reinforces NR by prolonging its lifetime, the essential physics behind these transitions can be understood by answering whether the polymer network could undergo sufficient stretching to produce SIC before the network breakdown through chain scission. The lifetime of the network competes with the timescale required for strain-induced crystallization, and the experimental timescale prescribed by the stretch rate is the third timescale. The competition among these timescales exhibits itself in the form of these abrupt transitions.

Received 6th October 2025,
Accepted 4th December 2025

DOI: 10.1039/d5sm01019e

rsc.li/soft-matter-journal



## 1. Introduction

Elastomers are an important class of polymeric materials with a wide range of applications (rubber gloves, anti-vibration systems, conveyor belts, seals and gaskets, vehicle tires, *etc.*). Their mechanical performance is directly related to product lifespans, vehicle fuel economy and microparticle generation on the road due to tire wearing. Various molecular strategies have been developed to improve stretchability and increase toughness. One successful method recognizes the need to make homogeneous network structures. Uniform strand length created by crosslinking ends of multi-arm stars leads to efficient load bearing and high tensile strength.[1] The double network idea[2,3] has also been explored to improve mechanical characteristics of vulcanized rubber whereas successes seem more visible and remarkable[4,5] in the case of hydrogels. A third approach is to introduce a mechanism for strain-induced crystallization (SIC), which occurs in vulcanized natural rubber (NR),[6–8] making NR typically stronger and tougher than synthetic rubbers. Here SIC acts like crosslinking to allow more load-bearing strands to participate in resistance against the network stretching, in both notch-free and prenotched configurations.

*School of Polymer Science and Polymer Engineering, University of Akron, Akron, Ohio, 44325, USA. E-mail: swang@uakron.edu*

Prestretching a notch-free NR to various stretch ratios, Busse found[9] that the more prestretched specimens can better resist crack propagation upon introduction of a cut. This "anti-fracture-mechanics" behavior indicates that some strengthening mechanisms took place upon sufficient stretching – SIC emerged. Upon sufficient stretching, SIC emerges in NR, making it more crack resistant. For example, Thomas and Whittle reported[10] that tensile strength changed sharply within a twenty-degree window, depending on whether SIC took place. Like Smith,[11] Thomas and coworkers[10,12] viewed tensile rupture of notch-free elastomers[13,14] to be due to a crack growth process initiated from small flaws. By stretching prenotched NR specimens with various notch sizes Thomas showed[15] an abrupt transition at room temperature as the notch size $a$ changes from 0.5 to 1 mm: below a critical notch size $a_c$ the critical stress for fracture was significantly higher. This abrupt transition with respect to $a$ has since been extensively confirmed[12,16–19] in literature. We call it the notch-critical transition (NCT) in this paper. It was concluded that the persistent presence of SIC at notch tip,[17] as confirmed by X-ray diffraction measurements,[8,20] provides additional resistance to crack growth. Lack of persistent SIC at notch tip above $a_c$ makes NR remarkably less resistant to rapid crack propagation. Moreover, Hamed and coworker showed[21] that the NCT diminished upon incorporating a sufficient amount of carbon black that made it easier for SIC to take place. In a recent comprehensive study on both natural

rubber and *cis*-1,4-polyisoprene[18] NCT was also characterized as a function of temperature and stretch rate. However, the phenomenology of NCT is still only described at the empirical level of "what" happened. In other words, the accounts available are only descriptive and not sufficiently explanatory.

Past extensive studies of elastomeric rupture[11,13,14,22] and fracture[23–27] have produced a doctrine[28] within the energy-based Griffith's framework of fracture mechanics that relates high energy release rate G from elastomeric fracture to energy dissipation originating from polymer viscoelasticity. However, a new perspective[29,30] has recently emerged from spatially and temporally resolved polarized optical microscopic (str-POM) studies[31,32] that investigated polymer fracture behavior and revealed the hidden structure of fracture mechanics for polymeric materials. In this new picture, polymer fracture strength $\sigma_{F(inh)}$ and presence of stress comparable to $\sigma_{F(in)}$ in an extensive spatial region surrounding the fracture plane are the origin of high toughness; elastomers' lifetime, controlled by bond dissociation kinetics as a function of bond tension and temperature, controls when failure takes place. With this new framework, it is also possible to understand why NCT and several similar transitions occur in stretching of unnotched and prenotched NR.

We will show in Section 2 how the concept[29] of network failure through bond dissociation not only provides a mechanistic explanation for how and why NCT occurs in prenotched NR but also leads us to predict two more related transitions regarding NR's ability to resist crack growth with respect to temperature and stretch rate. Specifically, there is also a temperature-critical transition (TCT): NR's resistance to crack growth abruptly increases as temperature decreases below a critical temperature $T_c$. Moreover, by changing stretch rate, a rate-critical transition (RCT) emerges: NR is more crack resistant below a critical stretch rate. Finally, unnotched NR should also show a RCT.

After the theoretical rationalization of these NCT, TCT and RCT in Section 2, we present experimental results in Section, verifying that there are indeed these five transitions. NCT, TCT and RCT are all abrupt because the critical condition, whether characterized in terms of notch size, temperature, or strain rate, is governed by the competition between two timescales: $t_{SIC}$, the time required for SIC to develop, and $t_{ntw}$, the lifetime of the chain network. It depends on the applied rate where $t_{SIC}$ and $t_{ntw}$ meet. If the network breaks down before sufficient chain stretching can induce crystallization, natural rubber (NR) will either rupture prematurely in notch-free specimens or fail to gain the enhanced resistance to crack growth provided by SIC in prenotched specimens.

## 2. Phenomenological description of five abrupt transitions

### 2.1. Unnotched: two transitions with respect to temperature and rate

To understand the phenomenon of NCT, we need to first explore the effect of SIC on rupture of unnotched NR and ask whether an abrupt temperature-critical transition (TCT) should occur. Thomas and coworker[10,12] reported a smooth TCT in notch-free stretching without explaining why SIC does not occur above $T_c$ and whether this TCT could be sharp. Separately, there is no experimental report or theoretical prediction of whether there would exist an abrupt rate-critical transition (RCT) in rupture, *e.g.*, whether NR becomes stronger in an abrupt manner over a narrow range of stretch rate.

It is well known,[13] as summarized by Kinloch,[28] that non-crystalline styrene-butadiene rubber (SBR) is weaker at higher temperatures. Today, we interpret this temperature dependence of rupture as reflecting the activation nature of bond dissociation:[29,33] Elastomers' lifetime $t_{ntw}$ is shorter at higher temperatures (due to more available thermal energy for activation), causing stretch to terminate earlier by rupture. At a given temperature $t_{ntw}$ rapidly decreases with increasing bond tension and therefore with stretch ratio $\lambda$. Above $T_c$, because of decreasing stretchability, NR undergoes rupture before SIC could take place. SIC can only occur when NR is sufficiently stretched, and temperature governs the occurrence of SIC through its influence on $t_{ntw}$. At a fixed stretch rate, characteristics of rupture (given by $\sigma_b$ and $\lambda_b$) may depend sharply on temperature as we envision a competition between rupture and SIC. Once the applied rate is given, there would be only one temperature $T_c$ at which $t_{ntw}$ and $t_{SIC}$ meet, as shown Fig. 1a. Above $T_c$, *e.g.*, at $T_2$, stretching along the inclined solid line will first cross the lower dashed curve before reaching the steeper curve of $t_{SIC}$. Thus, rupture at $T_2 > T_c$ occurs without SIC. Below $T_c$, the stretch line first meets the SIC curve – SIC occurs before rupture. Such a TCT is depicted in Fig. 1b. SIC prolongs NR's lifetime so that further stretching takes place. Temperature change may also slightly affect $t_{SIC}$ – the effect is not depicted in Fig. 1a (for simplicity) because the conclusion remains the same. In short, once stretch rate is chosen, temperature variation amounts to the crossing point (labeled by the small open circle) moving around in the phase space of time *vs.* strain to meet the inclined solid line at the transition. To focus on the transition mechanisms, explanation for how SIC extends NR's lifetime is an important topic but beyond the scope of the present study.

The same reasoning based on Fig. 1a predicts that rupture may depend sharply on the applied stretch rate $\dot{\lambda}$, exhibiting an RCT, as shown in Fig. 1c. We do not consider cases where the rate is so high that SIC has no time to form.[34] There exists one stretch ratio where NR is about to rupture, and SIC is also about to form. This condition is met only by one rate, represented by the inclined solid line in Fig. 1a. NR reaches its lifetime when stretched more slowly (along the upper inclined dashed line) before it is stretched enough to experience significant SIC; when stretched faster, *i.e.*, above critical rate $\dot{\lambda}_c$ along the lower inclined dashed line, NR can undergo SIC because the higher rate allows the elastomer to stretch more without rupture. In summary, the newly available theoretical concept of elastomeric lifetime[29] allows us to anticipate not one but two abrupt transitions regarding rupture of unnotched NR.

The preceding analysis is based on a simplified scenario that does not consider cases of partial SIC. For example, with

 

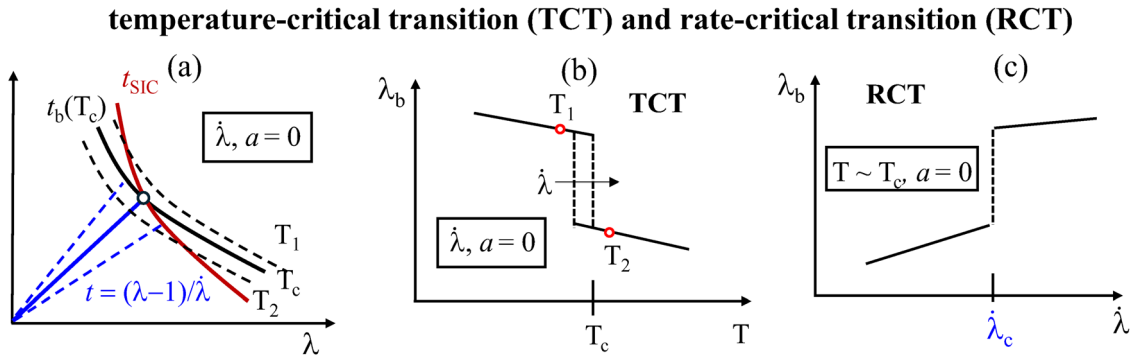


Fig. 1 (a) Two characteristic times, network lifetime $t_{ntw}$ and induction time $t_{SIC}$ for SIC, both decreasing with stretch ratio $\lambda$, represented by the two thick curves at temperature $T_c$. The two dashed curves indicate $t_{ntw}$ at two other temperatures below and above $T_c$. The two inclined dashed lines describe stretching at two other rates than the one represented by the inclined solid line. (b) Stretchability *vs.* temperature shows a sharp TCT, inferred from (a). (c) Stretchability *vs.* stretch rate shows a sharp RCT, also inferred from (a).

increasing stretch rate, a limited amount of SIC may emerge, leading to improved stretchability. Thus, the jump in $\lambda_b$ may not be remarkable. Conversely, if experiment reveals abrupt transitions, we may conclude that negligible SIC occurs below the transition. Throughout this paper, by "above (below) the transition," we mean that NR is stronger/tougher (weaker/less tough).

### 2.2. Prenotched NR: three transitions with respect to temperature, rate and notch size

**2.2.1. Transition with respect to rate and temperature.** There should be two similar abrupt transitions in prenotched NR. However, there is an obvious difference regarding network stretching in unnotched and prenotched specimens. Because of notch, significantly higher stretching is achieved at notch tip relative to stretching in the bulk (far field) so that the required network stretching for SIC occurs at a lower nominal strain and less stretching time. Consequently, the relationship between $t_{ntw}$ (and $t_{SIC}$) *vs.* nominal strain $L/L_0$ may switch such that slower stretching favors formation of SIC, as shown in Fig. 2a. In other words, there would be an opposite RCT, as shown in Fig. 2b. Paralleling Fig. 1a–c and 2b, c describe two abrupt transitions in prenotched NR, where the temperature effect is the same, *i.e.*, NR is tougher or more crack resistant at lower temperatures.

**2.2.2. Transition with respect to notch size.** The preceding analyses prepared us to address the original question of why an NCT is abruptly sharp. Like the other two transitions, the NCT is defined by a point in the time *vs.* strain phase space where three curves meet, as shown in Fig. 3. In other words, the NCT is determined by the applied rate, *i.e.*, by when the thicker inclined line meets the interception of the other two curves, marked by the middle open circle. For a larger notch with $a_2 < a_c$ the thick line meets the dashed curve ($a_2$) first, unless we adjust the stretch rate. In other words, we expect the NCT to occur at larger critical notch sizes ($a_c$) for slower stretching. Equivalently, according to Fig. 3a, as the stretch rate decreases, corresponding to the increase in the slope of the inclined lines, the NCT should monotonically shift to larger notch sizes, from $a_1$ to $a_2$. Similarly, we can predict that the NCT occurs at a smaller notch size as temperature rises for a fixed stretch rate. Upon temperature increase the $t_{ntw}$ curve in Fig. 3 would move to the left. This temperature effect may be compensated by using a smaller notch size. These two specific predictions regarding how the location of NCT, characterized by $a_c$,

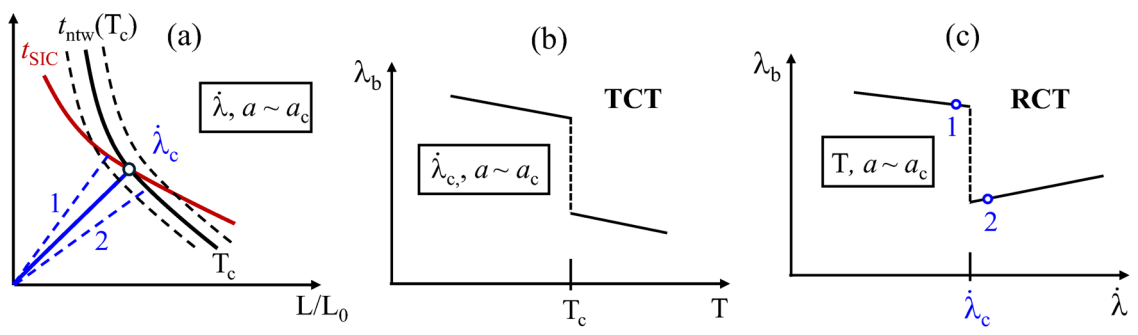


Fig. 2 (a) Two characteristic times $t_{ntw}$ and $t_{SIC}$, both decreasing with nominal stretch ratio $L/L_0$, represented by the two thick curves at temperature $T_c$. The two dashed curves indicate $t_{ntw}$ at two other temperatures below and above $T_c$. The two inclined dashed lines describe stretching at two other rates than the one represented by the inclined solid line. (b) Stretchability *vs.* temperature shows a sharp TCT, inferred from (a). (c) Stretchability *vs.* stretch rate shows a sharp RCT, also inferred from (a).

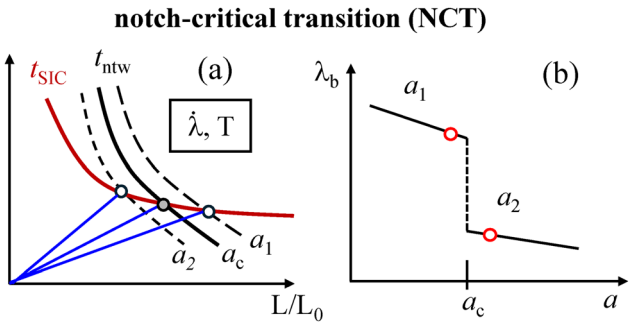


Fig. 3 (a) Two characteristic times $t_{ntw}$ and $t_{SIC}$, decreasing with nominal stretch ratio $L/L_0$, represented by the two thick curves at temperature $T_c$. The two dashed curves indicate $t_{ntw}$ at two other notch sizes, either smaller or larger than $a_c$. The two other inclined lines describe stretching at two other rates than the one represented by the middle line. (b) Stretchability *vs.* notch size shows a sharp NCT, inferred from (a).

changes with stretch rate and temperature are indeed in agreement with the recent extensive data[18] that illustrated the temperature and rate effects on the NCT.

**2.2.3. Persistent SIC at tip above NCT, RCT and TCT.** Based on our experimental results, we conclude that there is persistent SIC at notch tip above the transition that is either NCT, RCT or TCT. Fig. 4 elucidates a plausible scenario. Below the transition (*e.g.*, for either $a > a_c$, or $T > T_c$ or $e\,\dot{\lambda} > \dot{\lambda}_c$), no sufficient and sustainable SIC occurs at the notch tip. Once NR's strength is overcome at the onset of crack growth, there is no time for significant SIC at either crack tip or ahead of the tip in the bulk to prevent unstable fracture. Above the transition, SIC constantly develops at and ahead of the tip during continuous stretching so that fracture only occurs in the presence of SIC.

In summary, the three abrupt transitions arise from the competition between network breakdown *via* bond dissociation and the time-dependent development of SIC. Of these, only the notch-critical transition (NCT) has previously been explicitly recognized. In reality, three independent variables govern whether sustainable SIC can develop at a notch tip to enhance toughness: notch size, stretch rate, and temperature. When two of these variables are fixed, a sharp transition emerges as the third varies across a critical value. For example, at a given temperature and stretch rate, notch size can be adjusted until the condition for sustainable SIC at notch tip is met, leading to NCT.

Finally, we note that the NCT does not involve $a_c$ as large as 10 mm or as small as 0.1 mm. In prenotched systems, the chain network is more stretched at notch tip than in the bulk. This stretching intensification at notch tip increases with the magnitude of notch size $a$. There exists a characteristic length scale $P$ that determines the stretching state at notch tip. Recent str-POM observations[31,32] on non-crystalline elastomers indicate that $P$ may be in the range of 0.02–0.1 mm. Thus, for a large notch with $a$ = 10 mm critical nominal strain for SIC formation at notch tip would be so low that SIC cannot emerge elsewhere except at the notch tip – the scenario depicted in Fig. 4 would not take place. Our experiments in the next section indeed show that the critical value $a_c$ for NCT is *ca.* 1 mm at room temperature with a window of crosshead speed from 0.5 to 500 mm min$^{-1}$, and notch size of $a$ = 3 mm would simply be already too large (*cf.* Fig. 9b) for the region ahead of notch tip to develop SIC.

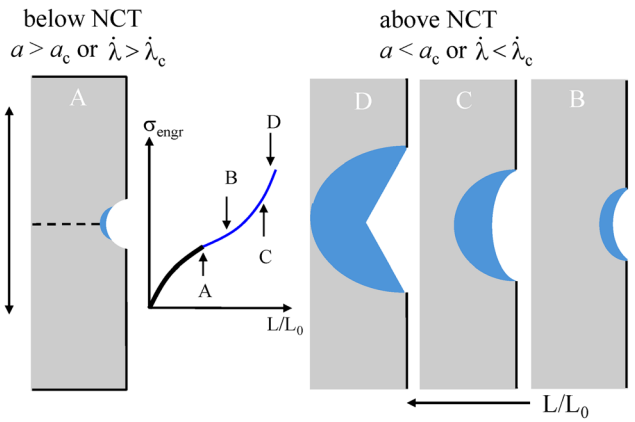


Fig. 4 Depiction of a notch-critical transition (NCT). Below the NCT, *i.e.*, for $a > a_c$, rapid fracture occurs at point A with minimal strength improvement at notch tip because SIC is essentially absent. At $a < a_c$ when the applied stretch rate is slow enough to permit significant SIC, crack growth does not occur until point D when crack propagation occurs in the presence of significant SIC.

### 2.3. Rate switching

To verify the scenario described in Fig. 4, we can carry out rate-switching tests. Referring to Fig. 4, if fast stretching produces fracture at point A, and a low rate does so at point D, we can apply the low rate to past point A and switch at points B and C respectively to the high rate. Rate-switching should also be instructive to elucidate the nature of RCT in unnotched NR. Such rate-switch tests will be presented in the following Section 4.3.

## 3. Sample preparation and testing method

Natural rubber (NR) gum, identified as SMR L, was supplied by Akrochem Corporation. Compounding was performed on a two-roll mill by incorporating 1 phr dicumyl peroxide (DCP) into the NR matrix. The compounded sheets were subsequently cross-linked by heat compression molding at 160 °C for 60 min.

All specimens were prepared by cutting from large sheet with a dogbone shaped die with a gauge length of 10 mm for both unnotched and notched experiments. The gauge width was 4 mm for unnotched samples and 8 mm for notched specimens. Stretching tests involve mounting such specimen onto two clamps separated by 33 mm. Notches were introduced by pushing a razor blade into the samples, and the resulting notch length was subsequently measured under microscope. Tensile testing was carried out using an Instron 5567 tensile

 

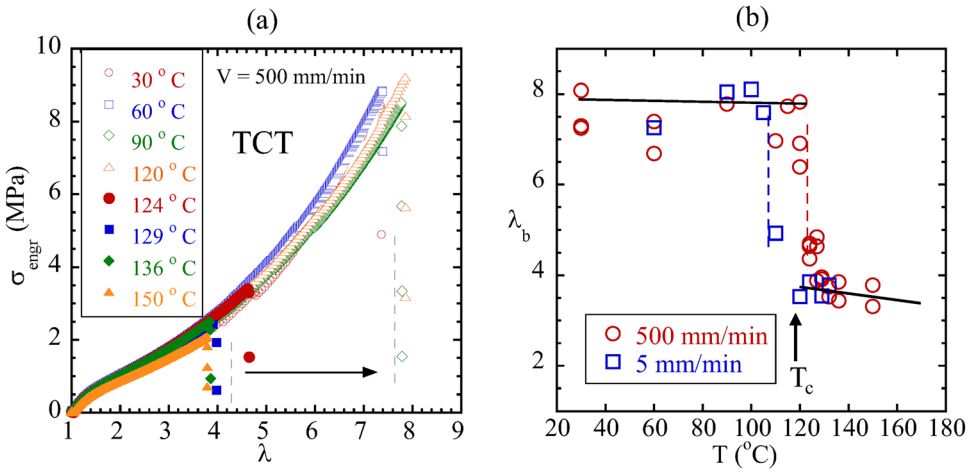


Fig. 5 (a) Engineering stress *vs.* stretch ratio of unnotched NR in uniaxial extension at eight different temperatures. Dogbone shaped specimens are stretched by moving the first clamp with a speed of $V$ = 500 mm min$^{-1}$ while fixing the second. (b) Stretch ratio $\lambda_b$ at rupture as a function of temperature for two speeds of 500 and 5 mm min$^{-1}$ respectively. The two TCT occurs respectively at *ca.* 120 and 105 °C, separated by *ca.* 15 degrees.

tester equipped with an environmental chamber for above ambient temperature testing.

## 4. Experimental results

### 4.1. Two rupture transitions in unnotched NR

According to the analyses in Section 2.1, SIC can result in two abrupt rupture transitions when we vary either temperature or stretch rate for continuous stretching of notch-free NR. Fig. 5a confirms the predicted abruptness of the TCT: NR is considerably more stretchable at and below 120 °C. At this highest crosshead speed of 500 mm min$^{-1}$, $T_c$ = *ca.* 120 °C. Fig. 5b shows TCT shifts to a lower temperature, *i.e.*, *ca.* 105 °C for slower stretching at 5 mm min$^{-1}$. In other words, the location of this sharp TCT, characterized by $T_c$ = 120 °C at $V$ = 500 mm min$^{-1}$, is not unique and shifts with the applied stretch rate, confirming the prediction depicted in Fig. 1b.

At 110 °C, as shown in Fig. 6a, NR indeed has a shorter lifetime and experiences rupture below stretch ratio of 4 at crosshead speed $V$ = 2.82 mm min$^{-1}$, which is apparently a level of network stretching insufficient to have enough SIC. The RCT emerges because an elastomer is more stretchable when stretched fast. With sufficient stretching at fast rates SIC emerges to enable further NR stretching; at low stretch rates, NR may suffer rupture before SIC emerges to reinforce the network and delay rupture. Fig. 6b shows that stretchability $\lambda_b$ sharply improves with increasing stretch rate, consistent with the predicted RCT in unnotched NR specimens. The stretchability of NR depends on the competition between two timescales: time required to form SIC and time elapsed before network lifetime expires, both depend on the applied rate.

### 4.2. Three fracture transitions in prenotched NR

Analyses in Section 2.2 suggest that there should be two transitions for prenotched NR. Temperature affects the lifetime

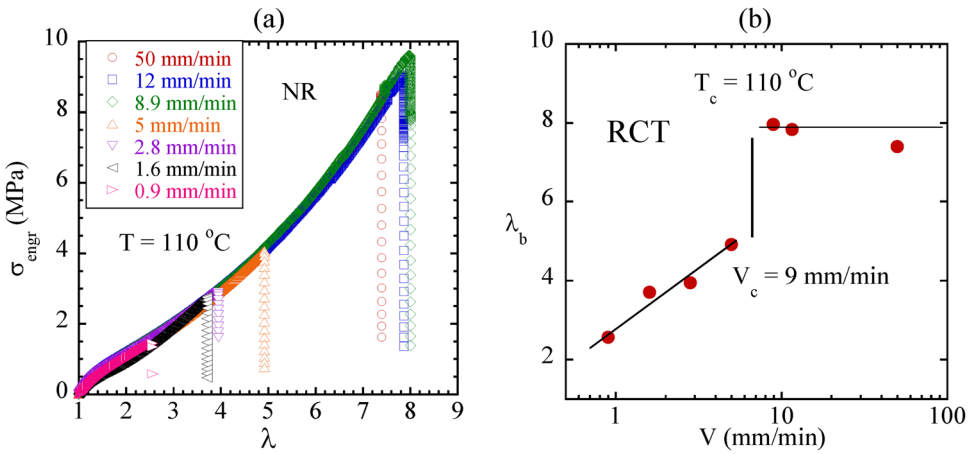


Fig. 6 (a) Stress *vs.* stretch ratio curves of unnotched NR in uniaxial extension at 110 °C obtained with different crosshead speeds. (b) NR becomes more stretchable when $V \geq$ 9 mm min$^{-1}$, showing an abrupt RCT at *ca.* 9 mm min$^{-1}$.

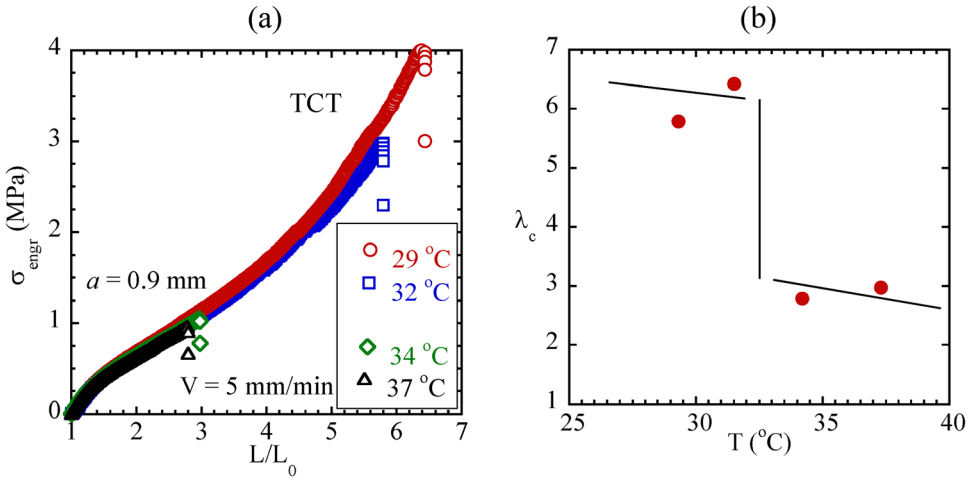


Fig. 7 (a) Stress *vs.* stretch ratio curves of prenotched NR with $a$ = 0.9 mm at a constant crosshead speed $V$ = 5 mm min$^{-1}$ at four temperatures, two below and two above the TCT. (b) NR becomes more crack resistant when $T \leq$ 32 °C, showing an abrupt TCT at *ca.* 32 °C.

$t_{ntw}$ of NR at notch tip in the same way as in unnotched cases, *e.g.*, NR is less resistant against fracture at higher $T$. Arguments based on the plots in Fig. 2a predict a sharp TCT, as shown in Fig. 2b, for a given notch size in the vicinity of $a_c$. Specifically, once the stretch rate is chosen along with $a_c$, lower temperatures favor the formation of SIC. This expectation is borne out as shown by Fig. 7a and b.

Separately, there is also a "reversed" RCT in prenotched NR. Contrary to the RCT in unnotched NR shown in Fig. 6b, slower stretching gives prenotched NR a better chance to develop SIC at the notch tip, as shown in Fig. 8a and b. These results confirm the prediction of RCT in Section 2.2.

To show how and why NCT is remarkably sharp, we change the notch size by a few percent, to demonstrate the emergence of an NCT in prenotched NR. As shown in Fig. 9a, at $a$ = 1.30 mm fracture occurs suddenly when the prenotched NR is stretched past $L/L_0$ = 2.5. The fracture is rupture like, with the breaking process finishing within one frame, *i.e.*, 1/30 of a second, as shown in Movie S1 in SI. However, stretching at $a$ = 1.24 mm continues to a much higher nominal strain before fracture. The crack propagation took seven frames to produce a final separation at $L/L_0$ = 4.8, as shown in Movie S2 in SI. The crack speed of $a$ = 1.24 mm is lower than that below the NCT at $L/L_0$ = 2.5 ($a$ = 1.3 mm) by at least a decade. Thus, upon reducing the notch size by just 5% from 1.30 mm to $a$ = 1.24 mm, NR has become far more crack resistant at the same applied stretch rate.

It is tempting to suggest that sufficient SIC emerged at the blunted tip to inhibit fracture from taking place past $L/L_0$ = 2.5 upon a 5% reduction in notch size. In other words, below the NCT at $a$ = 1.3 mm, SIC at notch tip is insufficient to prevent chain scission from producing rapid crack growth beyond $L/L_0$ = 2.5. In contrast, above the NCT at $a$ = 1.24 mm, SIC at notch tip continues to develop so that the system remains crack resistant despite growing load. The development of SIC can be visualized by the birefringence patterns shown in Fig. 9(d). At $L/L_0$ = 2.5, the bulk birefringence patterns of both samples are

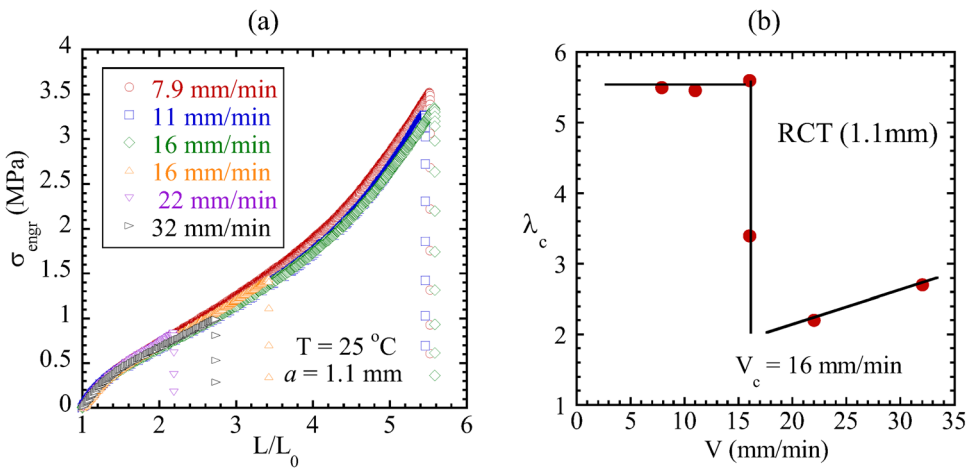


Fig. 8 (a) Stress *vs.* stretch ratio curves of prenotched NR with $a$ = 1.1 mm at 25 °C obtained with different crosshead speeds. (b) NR becomes more crack resistant when $V >$ 16 mm min$^{-1}$, showing an abrupt RCT at *ca.* 16 mm min$^{-1}$.

 

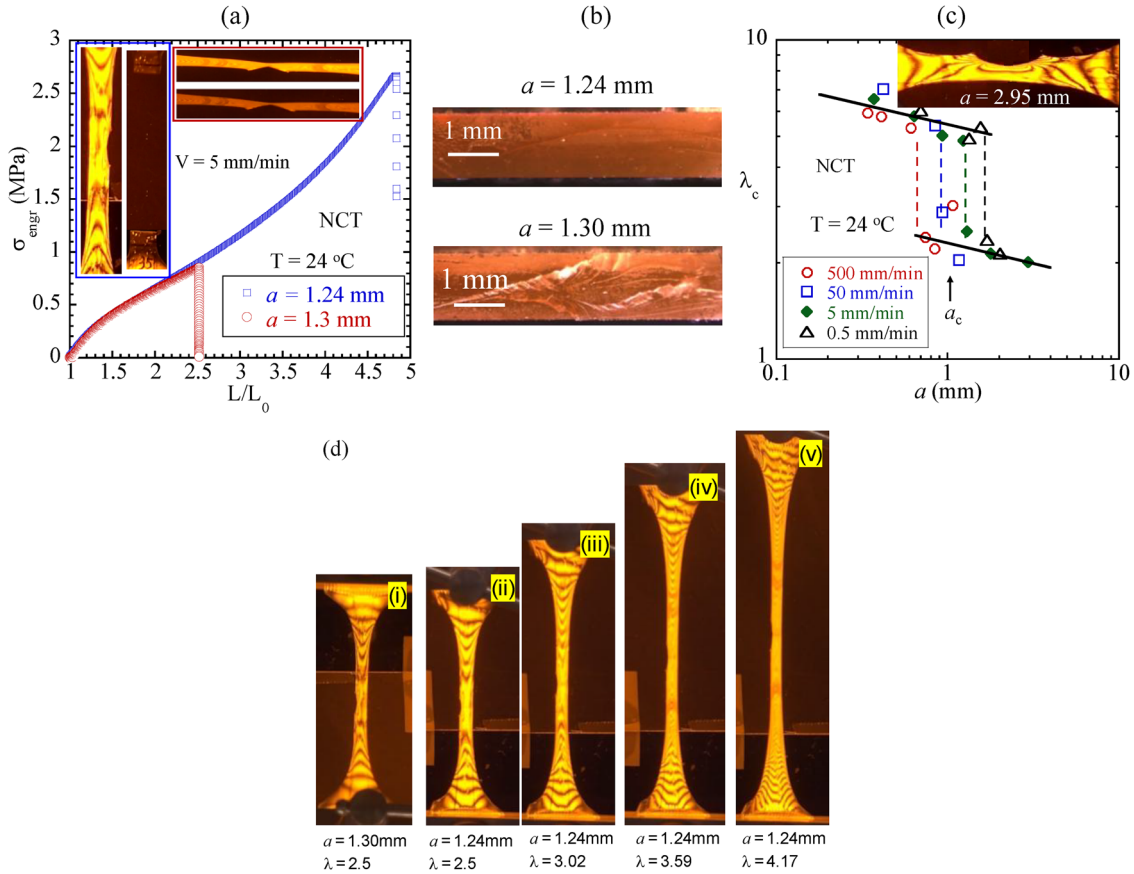


Fig. 9 (a) Stress *vs.* stretch ratio curves of two dogbone-shaped prenotched NR specimens containing notches of size $a$ = 1.24 and 1.30 mm respectively. At crosshead speed $V$ = 5 mm min$^{-1}$, at $a$ = 1.30 mm, it took *ca.* 612.23 s to reach rupture. Rupture started and finished in 1/30 s at nominal $L/L_0$ = 2.5, as shown by the two images in the blue box, taken by switching the specimen between two crossed polarizers. At $a$ = 1.24 mm, stretching continued well past 2.5 without crack propagation, and *ca.* 7 frames (7/30 s) elapsed before final breaking. Two images in the red box are separated by two frames, *i.e.*, 0.067 s, with the bottom being the last frame before total separation at *ca.* 1620 s. (b) Fracture surfaces of $a$ = 1.24 mm and $a$ = 1.30 mm with the former being smooth and the latter being rough. (c) The critical notch size for NCT decreases with increasing stretch rate. (d) Birefringence pattern of the two samples in (a) at various stretch ratios, which the disruption of birefringence pattern at the notch tip by SIC.

undistorted because SIC is negligible. Beyond 2.5, the pattern ($a$ = 1.24) became increasingly distorted, even away from the tip, reflecting increasing SIC. The phenomenon inspired the cartoons in Fig. 4 to depict what happens across the NCT, that are similar to that first proposed by[17] Rong and Hamed. As interpreted before,[17] for notch size $a < a_c$, SIC takes place at notch tip to prevent rapid crack growth; for notch size $a > a_c$, there is insufficient SIC to defer crack growth to higher nominal strain where SIC can occur ahead of the notch tip. With $V$ = 5 mm min$^{-1}$, at $a$ = 1.3 mm fracture occurs sharply across a critical stretch ratio (2.5) with exceedingly high crack propagation speed $v_c$ ($\sim$10 m s$^{-1}$), while stretching at $a$ = 1.24 mm continues to eventually reach $L/L_0$ = 4.8. The fracture about NCT took many frames to complete and produced a smoother fracture surface as shown in Fig. 9b. The much faster fracture at $a$ = 1.3 mm had a rougher surface; since it occurred at only $L/L_0$ = 2.5, there is insufficient network stretching in the bulk ahead of the notch tip to develop SIC.

This notch-critical transition (NCT) is remarkably sharp for other applied rates as well: changing the notch size by a few percent, prenotched NR undergoes the NCT at various critical values of $a_c$ as a function of stretching rate as shown in Fig. 9c. These four NCTs in Fig. 9b confirm our theoretical expectation (*cf.* first paragraph in Section 2.2.2) about the influence of stretch rate on the NCT. Filled diamonds in Fig. 9c indicate that the NCT is plausibly discontinuous.

In summary, we emphasize a key feature about these three (NCT, RCT and TCT) transitions. Below these transitions, the fracture instantly occurs at a considerably lower $\lambda_c$, and the fracture surface is rough. Above these transitions, the crack growth from the prenotch is usually much slower, ten and perhaps hundred times slower than it is below the transitions even though fracture occurs at significantly higher $\lambda_c$, characterized by relatively smooth fracture surfaces. Apparently SIC has the effect of increasing the network (load-bear) strand density so that the path of fracture is no longer tortuous.

Now we are returning to the question raised at the end of Section 2.2.2. The NCT is located around $a_c$ = 1 mm instead of 10 mm at room temperature for the range of applied stretch rate because fracture at significantly greater $a$ would occur

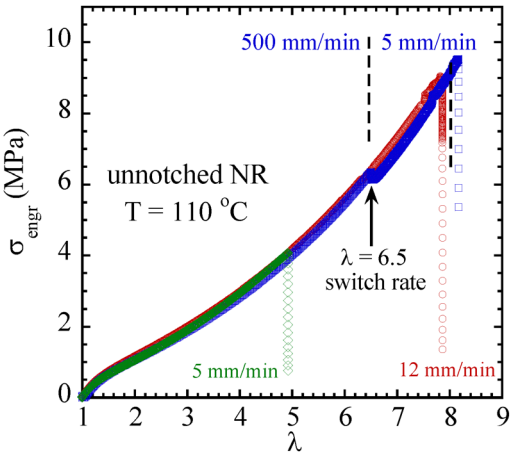


Fig. 10 Stress *vs.* stretch ratio curves of three NR unnotched dogbone-shaped specimens. Two of the samples were under continuous stretch at constant speed of 5 mm $min^{-1}$ and 12 mm $min^{-1}$, respectively. The other was stretched at 500 mm $min^{-1}$ till $\lambda$ = 6.5 when NR was further stretched at a slower speed of 5 mm $min^{-1}$.

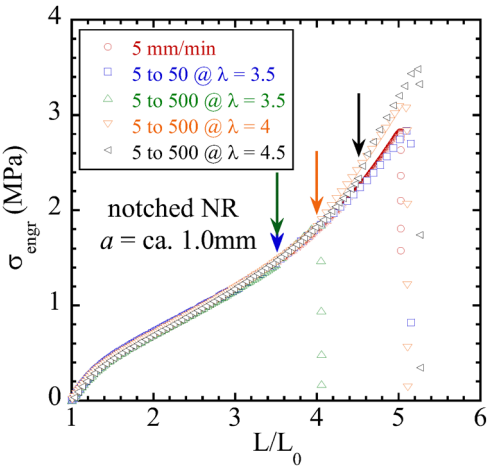


Fig. 11 Stress *vs.* stretch ratio curves of five NR notched dogbone-shaped specimens at $T$ = 25 °C. One specimen was under continuous stretch at constant speed of 5 mm $min^{-1}$ until fracture. The stretch speeds of the rest were switched from 5 mm $min^{-1}$ to 50 mm $min^{-1}$ or 500 mm $min^{-1}$ at various stretch ratios, *i.e.*, $L/L_0$ = 3.5, 4, 4.5. Vertical arrows indicate the stretch ratios, at which rate-switch took place.

without the far field undergoing sufficient stretching to cause SIC in the bulk – no transition occurs in absence of SIC. Image in Fig. 9b reveals clear birefringence fringe orders ahead of notch tip, indicating that there was no SIC in the bulk at rupture for $a$ = 3 mm let alone $a$ = 10 mm. Conversely, when $a$ is as small as 0.1 mm, there is little stress intensification at notch tip; when SIC occurs at the tip, it also takes place ahead of the tip. As confirmed by all data in Fig. 7, 8 and 9, NR is indeed always tough for $a \ll 0.6$ mm.

### 4.3. Rate-switch tests

Rate-switch experiments may effectively verify theoretical analyses in Fig. 1c regarding RCT in unnotched specimens and in Fig. 2c regarding fracture from pre-existing notch, along with the scenario depicted in Fig. 4. According to Fig. 6a, at 110 °C NR can only be stretched to $\lambda_b$ = 5 for crosshead speed $V$ = 5 mm $min^{-1}$. With $V$ = 500 mm $min^{-1}$ we can first stretch NR past 5 to $\lambda$ = 6.5 where SIC can take place so that rupture occurs above the RCT (*cf.* Fig. 5a). Then we lower $V$ to 5 mm $min^{-1}$ at 6.5. Instead of immediate rupture, the sample survives until $\lambda$ = 8.2 as shown in Fig. 10. Thus, this rate-switch supports the idea that sufficient SIC has strengthened the specimen at $\lambda$ = 6.5, allowing further stretch to continue. Beyond 6.5, the slow stretching favors further SIC, resulting in a specimen as strong as (if not stronger) revealed by the fast-stretching test with $V$ = 500 mm $min^{-1}$.

Based on prenotched NR samples of $a$ = *ca.* 1 mm, we carried out several rate-switch tests, with stretch speed $V$ = 5 mm $min^{-1}$ and $V$ = 500 mm $min^{-1}$ as the baselines, under which NR is either above the RCT, with stretching ratio reaching $\lambda_c$ = 5 or below the RCT, with $\lambda_c$ below 3 (*cf.* Fig. 8b). When rate-switching from $V$ = 5 to 500 mm $min^{-1}$ was made at $\lambda$ = 3.5, the sample underwent rapid fracture at around $\lambda_c$ = 4 (up-pointed triangles), unable to reach 5, as shown in Fig. 11. Unlike fracture above RCT, macroscopic separation was instant – the fracture was below RCT because significant SIC had not developed at 3.5. The outcome of this rate-switch test thus supports the depiction in Fig. 4 that SIC may have not sufficiently developed ahead of the notch tip, *e.g.*, at stage B. On the other hand, by comparison, rate-switch from $V$ = 5 to 50 mm $min^{-1}$ allows the sample to reach $\lambda_c$ = 5 – the subsequent stretching at $V$ = 50 mm $min^{-1}$ is apparently slow enough for SIC to keep forming at the tip, a scenario also consistent with descriptions of Fig. 2a, c and 4. Finally, when we switched rate from $V$ = 5 mm $min^{-1}$ to 500 mm $min^{-1}$ at higher strains, *i.e.*, $\lambda$ = 4 and 4.5, the prenotched NR appeared as tough as it showed at constant $V$ = 5 mm $min^{-1}$.

## 5. Conclusions

We carried out detailed experimental investigations to examine a well-known fracture transition in NR that we termed notch-critical transition (NCT): as the notch size decreases across a characteristic value of *ca.* 1 mm, the prenotched NR can turn much tougher in an abrupt manner (*cf.* Fig. 9a–c). Our recent KTBD of elastomeric fracture enables us to explain in Section 2 for the first time why this NCT is abruptly sharp. Analogously, unnotched NR undergoes a weak-to-strong transition (*cf.* Fig. 5a and b) that is also abrupt at a critical temperature $T_c$ and labeled as temperature-critical transition (TCT) in this paper. Both NCT and TCT occur because SIC can form under conditions that take NR above the transitions, making NR more resistant to stretching. When NR suffers enough chain scission due to stretching before being stretched sufficiently to develop SIC, it undergoes rupture like non-crystalline elastomers.

The KTBD also permits us to predict a new transition for unnotched NR, which is observed when the stretch rate is varied at elevated temperatures (*cf.* Fig. 6a and b). At sufficiently high temperatures NR may undergo rupture without SIC

 

formation – when it is slowly stretched it cannot be sufficiently stretched for SIC before rupture. We call this phenomenon rate-critical transition (RCT). We predict that RCT occurs in pre-notched NR as well. Here the RCT is reversed (*cf.* Fig. 8a and b). Slower stretching favors SIC formation at notch tip and results in tougher response of NR, because of the same competition between time required for SIC ($t_{SIC}$) and lifetime ($t_{ntw}$) of the chain network. RCT, TCT and NCT all occur because $t_{SIC}$ and $t_{ntw}$ decrease with nominal strain in quantitatively different ways.

## Author contributions

Zehao Fan: visualization, methodology, data curation, formal analysis. Fengjia Liu: data curation. Shi-Qing Wang: conceptualization. Writing – original draft. Writing – review & editing. Validation, supervision, methodology, investigation, funding acquisition, formal analysis.

## Conflicts of interest

There are no conflicts of interest to declare.

## Data availability

The authors state that the data underpinning the studies' findings are included in the article. Raw data supporting the study's findings can be obtained from the corresponding author upon request.

## Acknowledgements

This work is supported, in part, by the Polymers program through Special Creativity Extension of the US National Science Foundation grant DMR-2210184. The authors thank Akrochem Corporation for providing gum NR.

## References

1 S. Nakagawa, D. Aoki, Y. Asano and N. Yoshie, *Adv. Mater.*, 2023, **35**, 2301124.
2 P. Santangelo and C. Roland, *Rubber Chem. Technol.*, 1994, **67**, 359–365.
3 P. Santangelo and C. Roland, *Rubber Chem. Technol.*, 1995, **68**, 124–131.
4 J. P. Gong, Y. Katsuyama, T. Kurokawa and Y. Osada, *Adv. Mater.*, 2003, **15**, 1155–1158.
5 J. Yang, K. Li, C. Tang, Z. Liu, J. Fan, G. Qin, W. Cui, L. Zhu and Q. Chen, *Adv. Funct. Mater.*, 2022, **32**, 2110244.
6 G. Mitchell, *Polymer*, 1984, **25**, 1562–1572.
7 S. Murakami, K. Senoo, S. Toki and S. Kohjiya, *Polymer*, 2002, **43**, 2117–2120.
8 M. Tosaka, S. Murakami, S. Poompradub, S. Kohjiya, Y. Ikeda, S. Toki, I. Sics and B. S. Hsiao, *Macromolecules*, 2004, **37**, 3299–3309.
9 W. Busse, *Ind. Eng. Chem.*, 1934, **26**, 1194–1199.
10 A. Thomas and J. Whittle, *Rubber Chem. Technol.*, 1970, **43**, 222–228.
11 T. L. Smith, *Rubber Chem. Technol.*, 1978, **51**, 225–252.
12 C. Bell, D. Stinson and A. Thomas, *Rubber Chem. Technol.*, 1982, **55**, 66–75.
13 T. L. Smith, *J. Polm. Sci.*, 1958, **32**, 99–113.
14 T. L. Smith, *J. Polym. Sci., Part A: Gen. Pap.*, 1963, **1**, 3597–3615.
15 A. G. Thomas, *Physical Basis of Yield and Fracture: Conference Proceedings*, ed. A. C. Stickland, The Institute of Physics and the Physical Society, London, 1966, p. 134.
16 G. Hamed and B. Park, *Rubber Chem. Technol.*, 1999, **72**, 946–959.
17 G. Rong, G. Hamed and J. Jiang, *Rubber Chem. Technol.*, 2016, **89**, 631–639.
18 K. Tsunoda, Y. Kitamura and K. Urayama, *Soft Matter*, 2023, **19**, 1966–1976.
19 T. T. Mai, K. Tsunoda and K. Urayama, *J. Mech. Phys. Solids*, 2024, 193.
20 S. Trabelsi, P.-A. Albouy and J. Rault, *Macromolecules*, 2002, **35**, 10054–10061.
21 G. R. Hamed and A. A. Al-Sheneper, *Rubber Chem. Technol.*, 2003, **76**, 436–459.
22 H. Greensmith, *J. Appl. Polym. Sci.*, 1960, **3**, 175–182.
23 H. W. Greensmith and A. Thomas, *J. Polym. Sci.*, 1955, **18**, 189–200.
24 L. Mullins, *Trans. Inst. Rubber Ind.*, 1959, **35**, 213–222.
25 H. Greensmith, L. Mullins and A. Thomas, *Trans. Soc. Rheol.*, 1960, **4**, 179–189.
26 A. Thomas, *Rubber Chem. Technol.*, 1994, **67**, 50–67.
27 K. Tsunoda, J. Busfield, C. Davies and A. Thomas, *J. Mater. Sci.*, 2000, **35**, 5187–5198.
28 A. J. Kinloch and R. J. Young, *Fracture behaviour of polymers*, Springer Science & Business Media, 2013.
29 S.-Q. Wang, Z. Fan, C. Gupta, A. Siavoshani and T. Smith, *Macromolecules*, 2024, **57**, 3875–3900.
30 S.-Q. Wang, *Phys. Polym. Mech.*, 2025.
31 T. Smith, C. Gupta, Z. Fan, G. J. Brust, R. Vogelsong, C. Carr and S.-Q. Wang, *Extreme Mech. Lett.*, 2022, **56**, 101819.
32 Z. Fan and S.-Q. Wang, *Extreme Mech. Lett.*, 2023, **61**, 101986.
33 Z. A. Siavoshani, M. Yang, S. Liu, M.-C. Wang, J. Liu, W. Xu, J. Wang, S. Lin and S.-Q. Wang, *Soft Matter*, 2024, **20**, 7657–7667.
34 D. Villars, *J. Appl. Phys.*, 1950, **21**, 565–573.